prx-1 functions cooperatively with another *paired*-related homeobox gene, *prx-2*, to maintain cell fates within the craniofacial mesenchyme

Mei-Fang Lu[1], Hui-Teng Cheng[1], Michael J. Kern[2], S. Steven Potter[3], Bao Tran[4], Thomas G. H. Diekwisch[4] and James F. Martin[1,*]

[1]Alkek Institute of Biosciences and Technology, Center for Cancer Biology and Nutrition, Department of Medical Biochemistry and Genetics, Texas A&M University, Houston, TX 77030, USA
[2]Department of Cell Biology and Anatomy, Medical University of South Carolina, Charleston, 171 Ashley Avenue, SC 29425, USA
[3]Division of Basic Science Research, Children's Hospital Research Foundation, Cincinnati, 3333 Burnett Avenue, OH 45229, USA
[4]Department of Biomedical Sciences, Baylor College of Dentistry, 3302 Gaston Avenue, Dallas, TX 75246, USA
*Author for correspondence (e-mail: Jmartin@ibt.tamu.edu)

SUMMARY

The *paired*-related homeobox gene, *prx-1*, is expressed in the postmigratory cranial mesenchyme of all facial prominences and is required for the formation of proximal first arch derivatives. We introduced *lacZ* into the *prx-1* locus to study the developmental fate of cells destined to express *prx-1* in the *prx-1* mutant background. *lacZ* was normally expressed in *prx-1^{neo}; prx-1^{lacZ}* mutant craniofacial mesenchyme up until 11.5 d.p.c. At later time points, *lacZ* expression was lost from structures that are defective in the *prx-1^{neo}* mutant mice. A related gene, *prx-2*, demonstrated overlapping expression with *prx-1*. To test the idea that *prx-1* and *prx-2* perform redundant functions, we generated *prx-1^{neo};prx-2* compound mutant mice. Double mutant mice had novel phenotypes in which the rostral aspect of the mandible was defective, the mandibular incisor arrested as a single, bud-stage tooth germ and Meckel's cartilage was absent. Expression of two markers for tooth development, *pax9* and *patched,* were downregulated. Using a transgene that marks a subset of *prx-1*-expressing cells in the craniofacial mesenchyme, we showed that cells within the hyoid arch take on the properties of the first branchial arch. These data suggest that *prx-1* and *prx-2* coordinately regulate gene expression in cells that contribute to the distal aspects of the mandibular arch mesenchyme and that *prx-1* and *prx-2* play a role in the maintenance of cell fate within the craniofacial mesenchyme.

Key words: *Paired*-related homeobox, Craniofacial development, Genetic redundancy, Mouse, *prx-1*

INTRODUCTION

Cell lineage analysis performed primarily in the avian system has demonstrated that the craniofacial skeleton derives primarily from two embryologic sources: the cranial neural crest (CNC) and the cranial paraxial mesoderm with a minor contribution from the occipital somites. The majority of the skull is crest-derived, although there is disagreement about the origin of the bones of the calvarium (Couly et al., 1993; Le Douarin et al., 1993; Noden, 1988). A migratory cell population that originates in the dorsal neural tube, the CNC, undergoes an epithelial-to-mesenchymal transition to form the ectomesenchyme of the craniofacial primordia.

The neural crest has a remarkable degree of plasticity, giving rise to many different cell types including cartilage and nervous tissue, as well as the ability to regenerate after surgical ablation (Couly et al., 1996). Recent experiments investigating the mechanisms underlying patterning of the cranial neural crest have provided evidence that the crest and neural tube are patterned independently (Couly et al., 1998). Ablation experiments, as well as heterotopic transplantation of neural fold using quail-chick chimeras, have shown that the cranial neural crest can be patterned independently of its *Hox* gene expression profile (Couly et al., 1996, 1998). Thus, the CNC has intrinsic patterning capacity.

The expression of a number of homeobox genes has been documented within the CNC-derived ectomesenchyme of the craniofacial primordia. Among these is *prx-1* (previously called *Mhox*) and *prx-2* (previously called *S8*) which are closely related members of the *paired*-related *(prx)* family of homeobox genes (Cserjesi et al., 1992; Kern et al., 1992). At 9.5 d.p.c., *prx-1* is expressed in the CNC-derived mesenchyme of the frontonasal process, as well as the first and second branchial arches. At this stage, *prx-1* is also expressed within a group of cells ventral to the eye that will form the maxillary process of the first branchial arch. At later stages, *prx-1* expression is maintained within the mesenchyme of the maxillary and mandibular processes of the first branchial arch. Expression of *prx-1* is extinguished in mesenchymal cells as differentiation is initiated (Cserjesi et al., 1992; Kern et al., 1992; Kuratani et al., 1994).

Inactivation of *prx-1* in mice demonstrated that it played a

central role in development of skeletal elements derived from the proximal aspects of the first branchial arch (Martin et al., 1995). This suggested that there may be other, redundant genes functioning in the unaffected regions of the *prx-1*-expressing craniofacial mesenchyme. To follow the developmental progression of cells that are fated to express *prx-1* in the *prx-1* mutant background, we introduced the *lacZ* gene into the *prx-1* locus. In *prx-1^neo^*; *prx-1^lacZ^* homozygous mutant embryos, we found that *prx-1*-expressing cells initially contributed normally but failed to be maintained in developing craniofacial skeletal elements derived from proximal first branchial arch mesenchyme. To test the possibility of genetic redundancy between the *prx-1* and *prx-2* in the craniofacial primordia, we generated *prx-1^neo^*; *prx-2* double mutant mice and found novel defects of the distal aspects of the first branchial arch. Using a transgene that distinguishes between groups of *prx-1*-expressing cells in the craniofacial primordia, we provide evidence that subpopulations of cells within the larger field of *prx-1* expression were reprogrammed to new fates. Our data show that *prx-1*, in cooperation with *prx-2*, function to stabilize and maintain cell fates within the craniofacial mesenchyme.

MATERIALS AND METHODS

Nomenclature

With the goal of simplifying vertebrate homeobox gene nomenclature, we now refer to *Mhox* and *S8* as *prx-1* and *prx-2,* respectively (Scott, 1992).

Generation of *prx-1^lacZ^* allele

The *prx-1^lacZ^* targeting vector was constructed by inserting the *lacZ* gene in frame into a unique *Stu*1 site at the 5′ end of the homeobox. A *pgkneo* resistance cassette was introduced 3′ of *lacZ* in the reverse transcriptional orientation. The 5′ arm was a 2.5 kb *Pvu*II-*Stu*I fragment and the 3′ arm was a 4.0 kb *Stu*I-*Eco*RI fragment. The targeting vector was flanked on the 5′ side by a pMCI-thymidine kinase gene (Mansour et al., 1988). The targeting vector was linearized with *Pme*I.

The *prx-1^lacZ^* targeting vector was electroporated into ES cells (AK7) using a Bio-Rad gene pulser (500 uF, 240 V) and the ES cells were plated on SNL76/7 cells and cultured under positive and negative selection using G418 and FIAU (McMahon and Bradley, 1990). Surviving clones were analyzed by Southern analysis to identify targeted clones (Ramirez-Solis et al., 1992). The four targeted clones were expanded and genomic DNA extracted and analyzed using 5′ and 3′ probes to verify the integrity of the *prx-1^lacZ^* targeted locus. Two of these clones were injected into 3.5 d.p.c. blastocysts to generate chimeras. One clone transmitted the mutation through the germline.

Genotyping of mice

To identify mice carrying the *prx-1* and *prx-2* mutations, Southern blot was performed on genomic DNA obtained from tail biopsies of neonatal and 10-day-old mice and from the yolk sacs of mouse embryos. To isolate genomic DNA, tissue was incubated in lysis buffer (10 mM Tris pH 8.0, 25 mM EDTA pH 8.0, 100 mM NaCl, 1% SDS, 0.2 mg/ml Proteinase K) at 55°C for 3 hours, followed by phenol-chloroform extraction and ethanol precipitation. Genomic DNA was digested with the indicated restriction enzyme and fractionated on a 0.7% agarose gel. Digested DNA was transferred to Zeta-Probe GT membranes and hybridized with *prx-1*- or *prx-2*-specific probes. To identify the *prx-1^lacZ^* mutant allele, genomic DNA was digested with *Eco*RI and *Eco*RV. Using the A probe for Southern

blots, the wild-type allele migrated at 3.5 kb while the mutant allele was 2.5 kb. Details of the *prx-1^neo^* targeting strategy have been described (Martin et al., 1995). The *prx-2* targeting strategy resulted in the deletion of the third exon which encodes the DNA binding domain and was shown to be a null allele. The details for generating and genotyping this allele will be published elsewhere (Kern et. al., submitted). The *prx-1^neo^*; *prx-2* double mutant phenotype was analyzed on a 129/Sv × C57bl/6 hybrid background. All phenotypes were 100% penetrant unless otherwise stated in the text.

Generation of transgenic mice

The *prx-1* transgenic mice will be described in more detail elsewhere (J. F. M., unpublished data). Briefly, the construct used to generate the transgenic mice analyzed in this paper contains 2.7 kb of *prx-1* 5′ flanking region which extends into the 5′ UTR of *prx-1* fused to the *lacZ* gene from the puc19 AUGlacZ plasmid, which contains its own initiator methionine (Cheng et al., 1993). Five transgenic lines have been generated with similar results to what is reported here.

Skeletal analysis

Skeletal preparations were performed essentially as described (Martin et al., 1995). The data presented here are based on the analysis of twelve *prx-1^neo^–/–; prx-2–/–* and nine *prx-1^neo^–/–; prx-2+/–* skeletons.

Histology

Mouse tissues were fixed in 4% paraformaldehyde overnight and then dehydrated through graded alcohols and embedded in paraffin. Paraffin blocks were sectioned at 7-10 μm and stained with hematoxylin and eosin.

Staining for β-gal

The expression of *lacZ* in developing tissues was detected essentially as described (Beddington et al., 1989).

In situ hybridization

Whole-mount and sectioned in situ hybridization was performed as described (Edmondson et al., 1994). Probes for *pax9* (Neubuser et al., 1997), *patched* (Goodrich et al., 1996), *prx-2* (Opstelten et al., 1991) and *prx-1* (Cserjesi et al., 1992) have been described previously.

RESULTS

Introduction of *lacZ* into the *prx-1* locus

In order to study the developmental progression of cells that are fated to express *prx-1* in the *prx-1* mutant mice, we targeted *lacZ* to the *prx-1* locus to generate the *prx-1^lacZ^* allele (Fig. 1). To do this, we made an in-frame fusion of *lacZ* to a unique *Stu*I site in the 5′ end of the homeobox (Fig. 1A,B). The targeting vector, which contained 6.5 kb of homology, was linearized and electroporated into embryonic stem (ES) cells. After positive and negative selection, 96 colonies were analyzed by Southern analysis (Fig. 1C). Four (approximately 1 in 25) targeted events were identified and two clones were injected into C57Bl/6J blastocysts to generate chimeras. One of these clones transmitted the *prx-1^lacZ^* allele through the germline.

To confirm that the *prx-1^lacZ^* allele was genetically identical to the previously described *prx-1^neo^* allele (Martin et al., 1995), we crossed these two lines and analyzed the phenotypes of *prx-1^neo^*; *prx-1^lacZ^* mice. The phenotype of these mutant mice was a phenocopy of the *prx-1^neo^* homozygous mutant mice (data not shown). From this, we conclude that the *prx-1^neo^* and *prx-1^lacZ^* are genetically comparable. We next performed an expression

analysis of the *prx-1lacZ* allele at multiple developmental time points to confirm that the *prx-1lacZ* allele was expressed similarly to the endogenous gene.

Expression analysis of the *prx-1lacZ* allele

At 9.5 days post coitum (d.p.c.), *lacZ* expression was detected in the rostral aspect of the mandibular process, as well as within cells ventral to the eye that will contribute to the proximal components of the first branchial arch skeleton (Fig. 2A). Expression of *lacZ* was most intense at the distal half of the mandibular process. At this stage, we also found that *lacZ* was expressed in the mesoderm of the forelimb bud (Fig. 2B). At 10.0 d.p.c., expression of *lacZ* was maintained in the mandibular and maxillary process but was now found in more proximally located cells around the first branchial groove that will give rise to the external acoustic meatus and the external ear structures (Fig. 2C,D). *lacZ* was intensely expressed in the facial structures at 11.5 d.p.c. in a manner that was consistent with the earlier expression pattern. Intense staining was detected in the forming maxilla and mandible as well as in the frontonasal process (Fig. 2E). At this time point and at 12.5 d.p.c. (Fig. 2F), *lacZ*-expressing cells could be seen in cells that prefigure the dermal bones on the lateral aspect of the head such as the squamosal. From this analysis, we conclude that the *prx-1lacZ* allele expresses in an identical fashion to the endogenous gene (Cserjesi et al., 1992; Kern et al., 1992; Kuratani et al., 1994).

lacZ expression is lost from a group of proximal first arch-derived cells

We next analyzed the expression of *lacZ* in the *prx-1neo; prx-1lacZ* mutant background. *lacZ* expression was similar in wild-type and mutant embryos at 10.5 and 11.5 d.p.c. (Fig. 3A,B and not shown). However, at 12.5 d.p.c. a dramatic decrease in *lacZ*-expressing cells was detected in a region of the craniofacial primordia destined to contribute to the squamosal and other proximal first arch derivatives (Fig. 3C,D). This group of cells normally gives rise to the structures that were abnormal or missing in the *prx-1neo* homozygous mutant mice (Martin et al., 1995). Thus, cells fated to express *prx-1* initially contributed normally to forming cranial structures in the *prx-1* mutant; however, at later time points, a subpopulation of *lacZ*-expressing cells was lost or stopped expressing *lacZ*. Thus, *prx-1* function is required for maintenance of *prx-1*-expressing cells in the proximal first arch mesenchyme. These defects were not observed in the distal components of the first arch suggesting that another gene was compensating for the loss of *prx-1* function in that mesenchyme.

prx-2 and *prx-1* are coexpressed in the craniofacial primordia

prx-2 is a closely related *prx* family member that has overlapping expression with *prx-1* in the mandibular process of the first branchial arch, as well as in other regions of the embryo (Leussink et

al., 1995). Additionally, *prx-2−/−* mice had normal skeletons suggesting that another gene may substitute for loss of *prx-2* function in the skeletal primordia (M. J. K., unpublished data). To confirm that *prx-1* and *prx-2* were coexpressed in craniofacial primordia, we performed in situ analysis on serial sections of mouse embryos, as well as whole-mount in situ analysis of similarly staged mouse embryos. At 10.5 d.p.c., we found that *prx-1* and *prx-2* are coexpressed in cells within the mandibular, maxillary and frontonasal processes (Fig. 4A,B,E,F). *prx-1* was expressed both more abundantly and more broadly at this stage. Although *prx-1* and *prx-2* were both expressed at high levels at the tip of the mandibular arch (Fig.
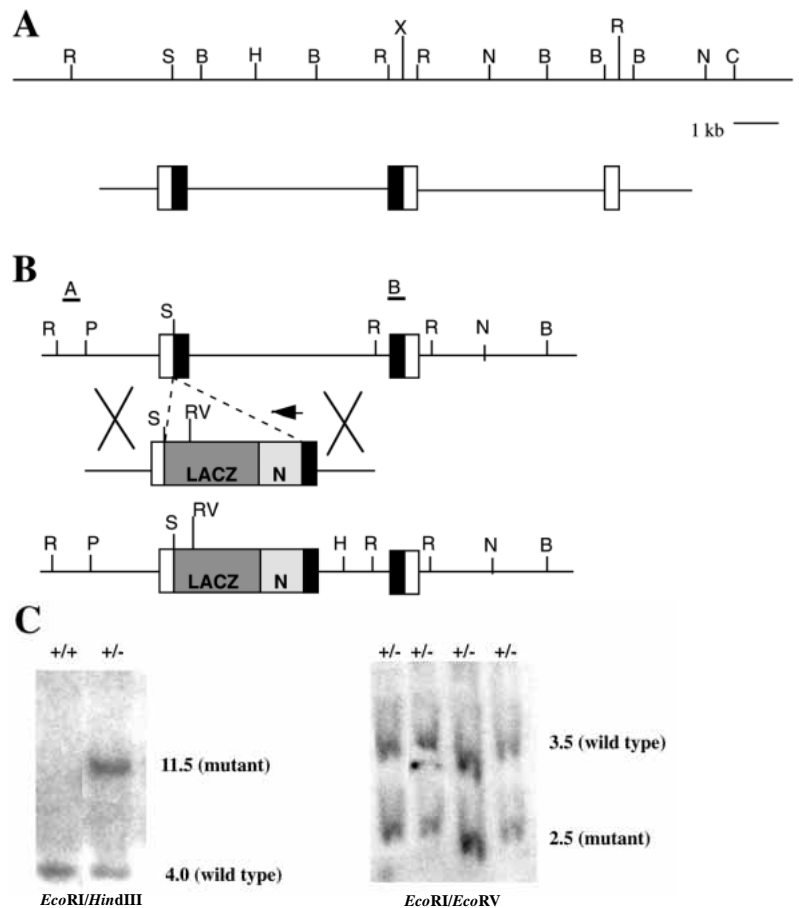

Fig. 1. Gene targeting strategy to introduce *lacZ* into the *prx-1* locus. (A) The top panel is a restriction map of the *prx-1* locus while the bottom panel shows the intron exon structure of the region of the *prx-1* gene containing the homeobox. The homeobox, shaded in black, is contained on two exons, denoted as boxes, with an intervening 4 kb intron. (B) At top is the wild-type allele with the targeting vector underneath. The bottom panel represents the structure of the mutant allele with the *lacZ* gene inserted in the homeobox of *prx-1*. The 5′ and 3′ probes are shown as horizontal lines above the wild-type allele. The arrow denotes the transcriptional orientation of the *Pgkneo* (N) cassette. With the introduction of *lacZ* into the *prx-1* locus a new *Eco*RV site has been inserted. Additionally, a *Hin*dIII site has been shifted more 3′. (C) Southern blot analysis of gene targeted ES clones digested with *Eco*RI and *Hin*dIII on the left and *Eco*RI and *Eco*RV on the right. The genotypes of each ES clone is shown at top. The control ES DNA is shown at the extreme left. For the *Eco*RI-*Hin*dIII digest, the A probe hybridizes to a wild-type fragment of 4.0 kb while the mutant fragment is 11.5 kb in length. For the *Eco*RI-*Eco*RV double digest, the wild-type fragment is 3.5 kb while the mutant is 2.5 kb in length. B, *Bgl*II; C, *Cla*I; H, *Hin*dIII; N, *Nco*I; R, *Eco*RI; RV, *Eco*RV; P, *Pvu*II; S, *Stu*I.
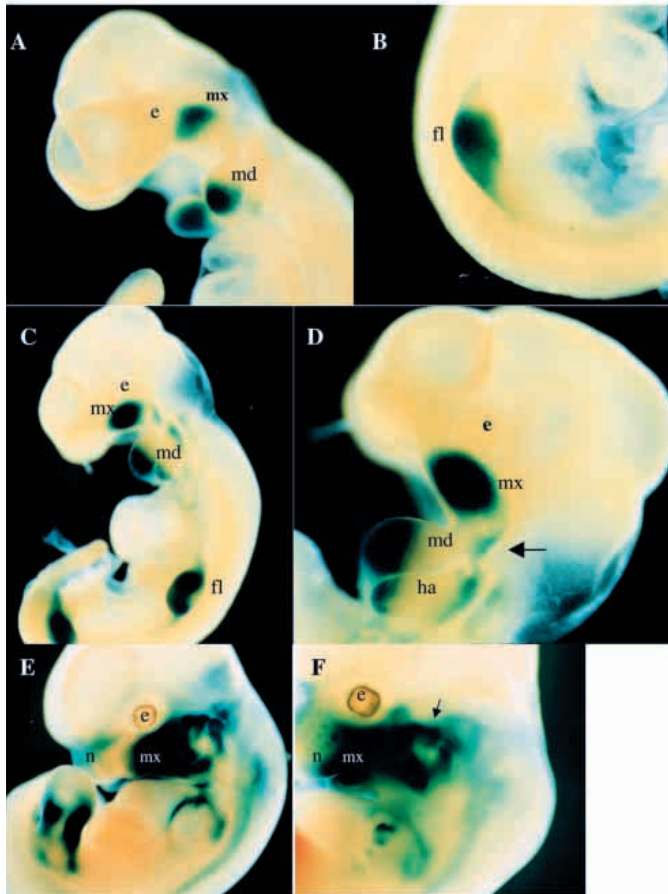
Fig. 2. Expression of the *prx-1^lacZ* allele during embryogenesis.
(A) Lateral view of 9.5 d.p.c. mouse embryo stained for β-gal
demonstrates expression in the forming maxillary (mx) and
mandibular (md) process. Note the expression of *lacZ* is highest at
the distal end of the mandibular process. (B) Close-up view of a 9.5
d.p.c. mouse embryo showing expression of *lacZ* in the mesoderm of
the developing forelimb (fl). (C,D) Lateral view at low magnification
(C) and high magnification (D) of a 10.0 d.p.c. mouse embryo
showing continued expression of *lacZ* in the mandibular and
maxillary processes as well as proximal expression in cells
surrounding the first branchial groove that will give rise to ear
structures (arrow). (E) Expression of *lacZ* at 11.5 d.p.c. Expression
can be seen in the forming maxilla and mandible as well as lower
levels of expression in the frontonasal process (n). The left forelimb
has been removed to show expression in the craniofacial structures.
(F) *lacZ* expression at 12.5 d.p.c. shows staining in maxilla and
mandible as well as external ear and cells that prefigure the dermal
bones at the lateral aspect of the head (arrow). e, eye; fl, forelimb
bud; ha, hyoid arch; md, mandibular process; mx, maxillary process.

4A,E), *prx-1* was also expressed at high levels in the proximal
mandibular process where prx-2 expression was less intense
(Fig. 4B,F). At 11.5 d.p.c., whole-mount in situ demonstrated
that expression of both *prx-1* and *prx-2* was maintained at high
levels in equivalent groups of cells in the mandibular and
maxillary processes (Fig. 4C,G). At 12.5 d.p.c., expression of
these two genes was downregulated in the mandibular process
but expression in the maxilla and nasal processes was
maintained (Fig. 4D,H). We identified some minor differences
in the craniofacial expression patterns of *prx-1* and *prx-2*. At
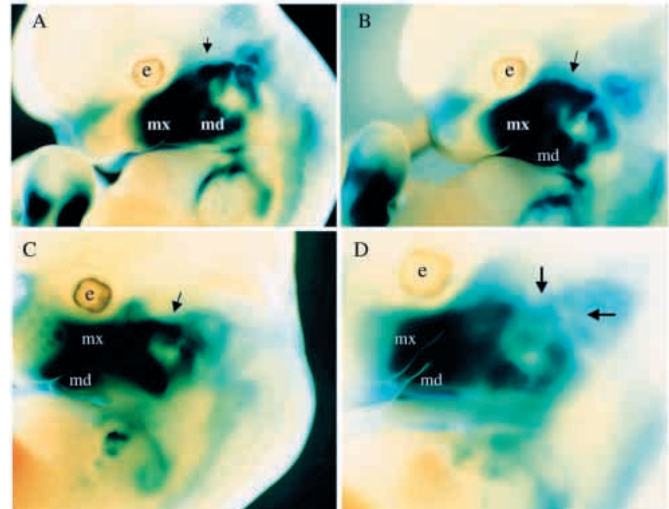

Fig. 3. *lacZ*-expressing cells contribute to but are not maintained in
the forming dermal bones of *prx-1^neo; prx-1^lacZ*mutants.
(A,B) Expression of *lacZ* at 11.5 d.p.c. in the wild type (A) and *prx-
1^neo; prx-1^lacZ* mutant (B) demonstrates that cells that are fated to
express *prx-1* are found in the cells that will give rise to the dermal
bones of the lateral skull as denoted by the arrow. (C,D) At 12.5
d.p.c., *lacZ*-expressing cells (arrow) are found in cells that are
forming membrane bones in the wild type (C), but in the *prx-1^neo;
prx-1^lacZ* mutant (D) *lacZ*-expressing cells have been lost from cells
that will form the lateral skull bones as shown by the arrows. e, eye;
md, mandible; mx, maxilla.

12.5 d.p.c., *prx-2* was expressed slightly more medially in the
frontonasal process than *prx-1* (Fig. 4D,H).

We examined expression of *prx-1* in the *prx-2* mutant mouse
to determine if there was a compensatory increase in *prx-1*
expression. No differences in expression of *prx-1* in the *prx-2*
mutants as compared to wild-type mice were detected (data not
shown). Similarly, expression of *prx-2* in the *prx-1^neo*
homozygous mutants was examined at 10.5 and 11.5 d.p.c. and
no differences were detected between wild type and mutant
(data not shown). Thus, *prx-1* and *prx-2* do not cross regulate
each others' expression.

prx-1^neo; prx-2 double mutant mice have severe defects of distal first branchial arch derivatives

To generate double mutant mice, we crossed *prx-1^neo*
heterozygotes to *prx-2* homozygous mutant mice which are
viable and fertile (M. J. K., unpublished data). The majority of
the analysis of double mutant mice was performed using the
prx-1^neo allele, although the phenotypes of *prx-1^neo; prx-2*
double mutants were identical to the *prx-1^lacZ; prx-2* double
mutants. Compound *prx-1^neo; prx-2* heterozygotes were viable
and fertile, and had normal skeletons. Intercrosses between
compound heterozygotes gave rise to doubly mutant neonatal
mice in the expected Mendelian ratios demonstrating that the
double mutants were able to progress through development
(data not shown). We found that one copy of the wild-type *prx-
1* allele was sufficient for skeletal development, since *prx-1^neo*
heterozygotes on the *prx-2* homozygous mutant background
were normal.

The double mutant neonates never fed, had respiratory
distress marked by gasping motions and cyanosis, and died

within 24 hours of birth. All double mutants had a cleft secondary palate, which was likely to contribute to their inability to feed and breathe (Fig. 5A-D). *prx-1neo; prx-2* double mutant neonatal mice had more hypoplastic and posteriorly displaced auricles than the *prx-1neo* homozygous mutant mice, as well as open eyes secondary to failure of eyelid formation (data not shown). Double mutant mice also had severe defects in limb morphogenesis. A detailed analysis of the limb phenotype will be presented elsewhere (Lu et al., 1998).

Skeletal preparations of neonates demonstrated that the mandible was severely shortened and fused at its most rostral aspect (Fig. 5E-H). Wild-type neonatal mice and *prx-1neo* mutants had well-formed mandibles connected by a symphysis at its rostral aspect (Fig. 5E,F). The *prx-1neo–/–; prx-2+/–* mice had a mandible that was fused rostrally and had only a single midline incisor tooth (Fig. 5G). *prx-1neo–/–; prx-2–/–* mice had a severely shortened mandible that was also rostrally fused and failed to form an incisor tooth (Fig. 5H). Thus, the mandibular and incisor tooth phenotypes were sensitive to the dosage of the *prx-2* gene. We also detected defects in the skull base of double mutants although these phenotypes were less severe than the mandibular defects (Fig. 5A-D). In double mutant mice, the palatal and zygomatic process of the maxilla were deleted (Fig. 5D). In *prx-1neo–/–; prx-2+/+* mice, the maxillary zygomatic process was intact and the palatal was reduced but present (Fig. 5B).

The primary cartilage of the mandibular process is Meckel's cartilage. This structure was more severely affected in double mutant embryos as demonstrated by cartilage staining at 14.5 d.p.c. At this stage, Meckel's cartilage is a well-defined, rod-shaped cartilage (Fig. 5I). In the *prx-1neo–/–; prx-2+/+* mice, Meckel's cartilage had an abnormal sigmoidal morphology (Fig. 5J) whereas *prx-2* mutants had a normal Meckel's cartilage. In the double mutant, Meckel's cartilage was absent except for a remnant at the most rostral tip of the developing mandible (Fig. 5K).

prx-1neo; prx-2 double mutants have abnormal mandibular incisor teeth

To further characterize the distal mandibular arch phenotype, we performed histological analysis of the developing teeth in double mutant embryos. In wild-type embryos at 12.5 d.p.c., the two incisor teeth had progressed from the bud stage to the early bell stage in which the base of the tooth bud had become invaginated by the underlying dental papilla (Fig. 6A). In the double mutants, mandibular incisor development arrested as a single tooth bud. Parasagittal and transverse sections through the double mutant incisor tooth bud demonstrated that, while mesenchyme had condensed around the dental epithelium, the morphogenetic events that lead to the bell-stage tooth failed to occur (Fig. 6B,C). Sections of embryos at 16.5 d.p.c. demonstrated the reduction in size of the tooth organ as well as epithelial hypertrophy and abnormal positioning of the tooth germ relative to the alveolar bone. In addition, there was a failure of odontoblasts and ameloblasts to differentiate (Fig. 6D,E).

We examined the expression of molecular markers that have been implicated in tooth formation. At 12.5 d.p.c., we examined the expression of *pax9* which has been demonstrated
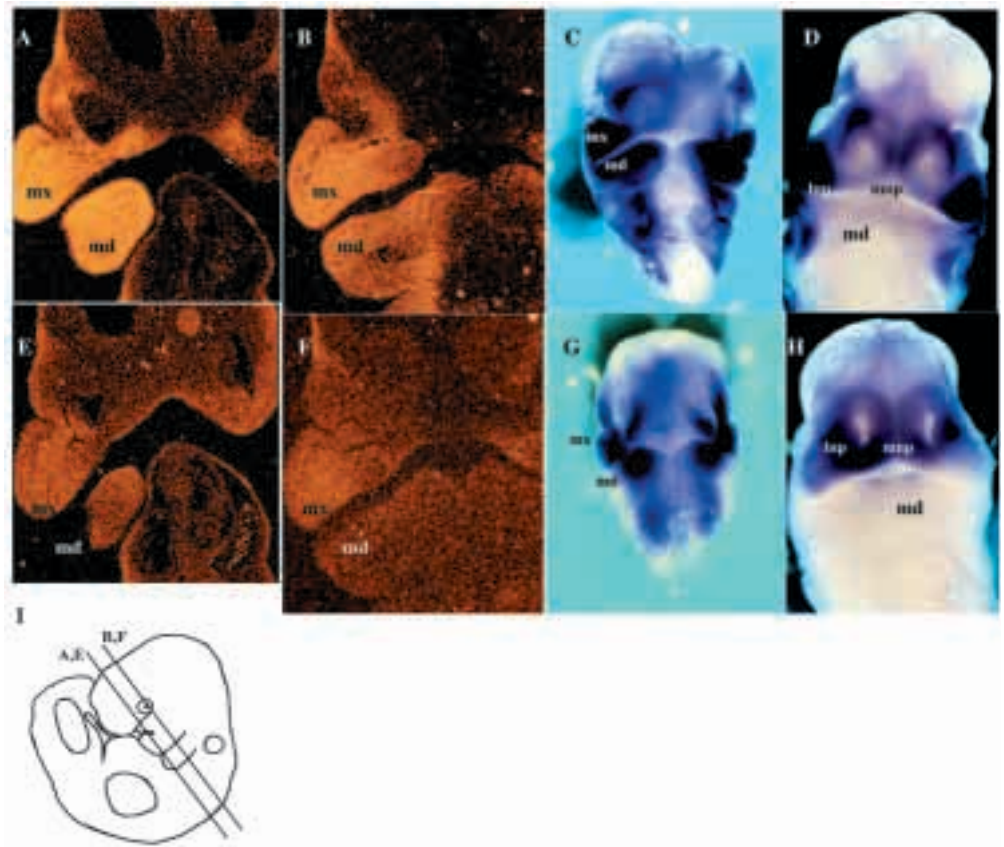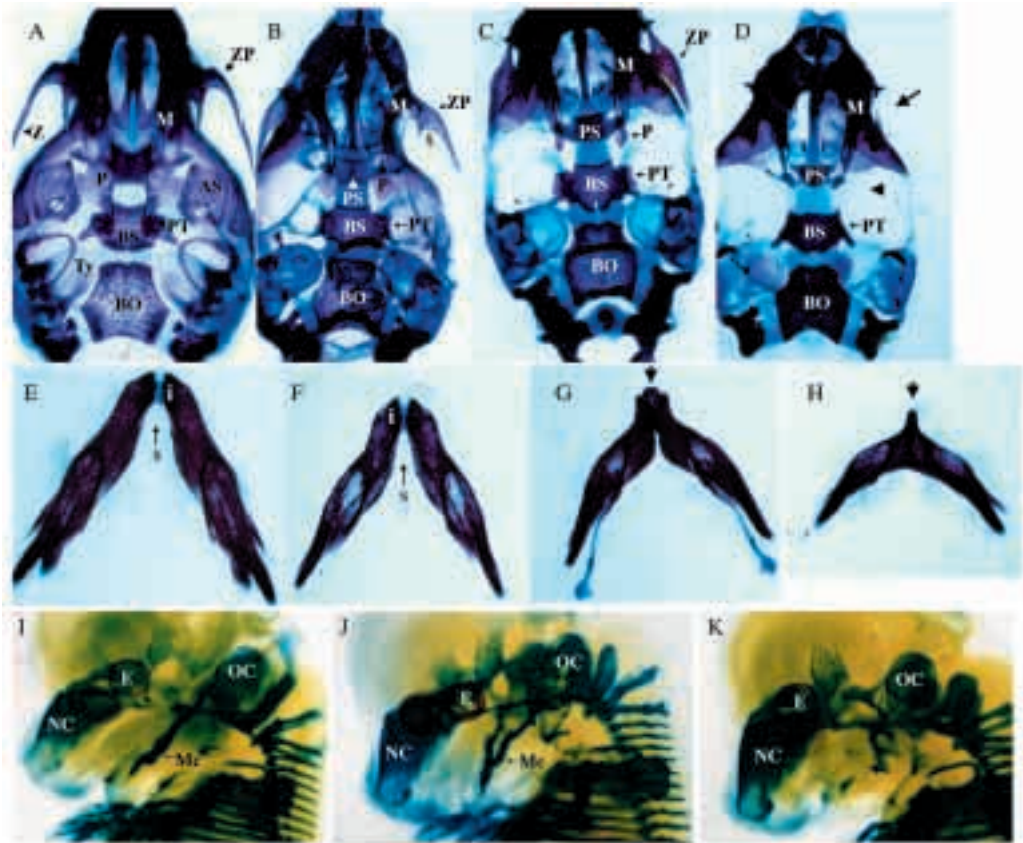

Fig. 4. *prx-1* and *prx-2* are coexpressed in the craniofacial regions of embryos at 10.5 d.p.c., 11.5 d.p.c. and 12.5 d.p.c. (A,B,E,F) In situ analysis using a *prx-1* (A,B) and *prx-2* (E,F) probe on serial sections through the craniofacial region of 10.5 d.p.c. embryos. (A,E) Note that *prx-1* and *prx-2* are coexpressed in the maxillary prominence (mx) and rostral aspect of the mandibular process (md). (B,F) Slightly more posterior sections through 10.5 mouse embryos demonstrates that *prx-1* and *prx-2* are coexpressed in these regions of the maxillary and mandibular processes, although *prx-2* expression is less abundant at these levels when compared to the more rostral sections in E. The level of sections is diagrammed in I. Whole-mount in situ demonstrating expression for *prx-1* (C,D) and *prx-2* (G,H) in developing embryos at 11.5 d.p.c. (C,G) and 12.5 d.p.c. (D,H). *prx-1* and *prx-2* are coexpressed in the mandibular and maxillary processes at 11.5 d.p.c. (C,G). At 12.5 *prx-1* and *prx-2* continue to be coexpressed in developing facial structures although *prx-2* is expressed at higher levels in the medial nasal process. Expression of both genes has been downregulated at this stage. Lnp, lateral nasal process; md, mandibular process; mnp, medial nasal process; mx, maxillary process.

Fig. 5. Craniofacial phenotypes of *prx-1ⁿᵉᵒ; prx-2* double mutant mice. (A-D) Skeletal preparations of neonatal skulls showing the base of the skull. The wild-type skull (A) shows the normal skull components stained in red for bone and blue for cartilage. The *prx-1ⁿᵉᵒ* mutant (B) demonstrates a number of abnormalities including reduced size of the palatal (P) and palatal process of the maxilla (M). This results in cleft of the secondary palate. The alisphenoid (AS), zygoma (Z) and tympanic ring (Ty) are missing in the *prx-1ⁿᵉᵒ* mutant. In the *prx-1ⁿᵉᵒ–/–; prx-2+/–* (C), the base of skull is slightly more severely affected in that the palatal is more reduced than in the *prx-1ⁿᵉᵒ–/–; prx-2+/+* skull. The double mutant base of skull (D) has complete absence of the palatal (arrowhead) as well as absence of the zygomatic process (ZP) of the maxilla (arrow). (E-H) Rostral view of dissected mandibles from neonatal mice stained for cartilage (blue) and bone (red). The wild-type mandible (E) shows the well formed dentary as well as two incisor teeth (i) at the rostral tip. The morphology of the mandible

from *prx-1ⁿᵉᵒ–/–* mice (F) is comparable to wild type, however, the dentary is slightly shortened and the incisors are normal. Mandible from *prx-1ⁿᵉᵒ–/–; prx-2+/–* (G) mice is fused rostrally and has a single incisor tooth (arrow). This phenotype is more severe in *prx-1ⁿᵉᵒ–/–; prx-2–/–* neonates in which the mandible is severely shortened and fused at the rostral tip. Additionally, the incisor is absent (arrow). (I-K) Embryos at 14.5 d.p.c. stained for cartilage. The wild type (I) shows the well-formed Meckel's cartilage (Mc) within the forming mandibular region. The morphology of Meckel's cartilage is moderately abnormal in the *prx-1ⁿᵉᵒ–/–* embryo (J), however, in the double mutant embryo (K) Meckel's cartilage is absent (arrow) except for a remnant at the most rostral tip of mandible. The malleus found at the proximal end of the forming mandible is still present in double mutant embryos. AS, alisphenoid; E, eye; BS, basisphenoid; BO, basioccipital; i, incisor tooth; M, maxilla; NC, nasal cartilage; OC, otic capsule; P, palatal; PT, pterygoid; s, symphysis; Ty, tympanic ring; Z, zygoma; ZP, zygomatic process.

to be expressed in dental mesenchyme of all tooth germs and is required for normal tooth development (Neubuser et al., 1997). In double mutant mandibular incisors, expression of *pax9*, was downregulated in comparison to wild type (Fig. 6F,G). In contrast, expression of *pax9* in molars was unaffected in the double mutant embryos. We also examined expression of *patched* which is expressed in developing teeth and is a component of the *Shh* signaling pathway (Helms et al., 1997; Marigo et al., 1996). We found that, as for *pax 9*, expression of *patched* was downregulated in the mandibular incisor tooth germ of double mutant embryos (Fig. 6H,I). These results demonstrate that *prx-1* and *prx-2* cooperatively function to maintain expression of *pax9* and *patched* in the forming mandibular incisor teeth.

To determine if the mesenchyme of the mandibular process had been correctly specified, we examined expression of *sox9*, which marks the prechrondrogenic mesenchyme of the branchial arches (Zhao et al., 1997; Thomas et al., 1997). At 11.5 d.p.c., *sox9* is expressed, prior to chondrogenesis in the cells that will form Meckel's cartilage in the mandibular process (Fig. 6J). In the double mutants at this stage, we found

that *sox9* was expressed normally (Fig. 6K). Thus, in the *prx-1ⁿᵉᵒ; prx-2* double mutant, the condensations are initiated normally, as determined by *sox9* expression, but fail to be maintained, as determined by the failure of Meckel's cartilage to form.

prx-1ⁿᵉᵒ; prx-2 double mutant craniofacial mesenchyme ectopically expresses a *prx-1* transgene

We sought to follow the developmental fate of cells destined to express *prx-1* in the double mutant background. For this purpose, we used a *prx-1* transgene that drives expression of *lacZ* in a subset of craniofacial precursors that normally express the endogenous *prx-1* gene (J. F. M., unpublished data). This transgene, called *prx-1 2.7 lacZ*, first expresses *lacZ* in the lateral aspect of the maxillary process at 11.5 d.p.c. At 12.5 d.p.c., *prx-1 2.7 lacZ* drives *lacZ* expression in the distal aspect of the developing mandible in addition to the lateral maxilla (Fig. 7C). Therefore, this transgene distinguishes between specific subsets of cells within the craniofacial primordia that would normally express *prx-1*. To follow the

developmental progression of these subpopulations of cells in the *prx-1neo−/−; prx-2−/−* mice, we crossed this transgene into the double mutant background.

At 10.5 d.p.c., the *prx-1 2.7 lacZ* transgene does not express in the craniofacial primordia of wild-type embryos (Fig. 7A). Expression of *lacZ* was first detected in a small group of cells in the wild-type maxillary process at 11.5 d.p.c.. In 10.5 d.p.c. double mutant embryos, *lacZ* was detected in the maxillary process, the distal tip of the mandibular process, as well as in the hyoid arch (Fig. 7B). Therefore, in the double mutant embryos, expression of *lacZ* was expressed prematurely in the maxillary and mandibular processes and ectopically in the hyoid arch. The *prx-1 2.7 lacZ* transgene does not express in the hyoid arch in wild-type embryos. In the wild-type 12.5 d.p.c. embryo, expression of *lacZ* was seen in the lateral aspect of the maxilla, as well as in cells at the distal tip of the mandible (Fig. 7C). In double mutant 12.5 d.p.c. embryos, *lacZ* expression was detected in ectopic locations in cells derived from the hyoid arch, as well as in proximally located cells surrounding the developing external ear structures. *lacZ* was also more broadly expressed in the forming mandible and maxilla of double mutant embryos (Fig. 7D). Thus, in the double mutant embryos, mesenchymal cells within the hyoid arch and cells around the forming external ear have acquired the characteristics of cells normally found within the maxillary and mandibular processes.

DISCUSSION

We have introduced *lacZ* into the *prx-1* locus and have found that *prx-1* mutant cells initially contributed normally but failed to be maintained in the structures that are defective in *prx-1neo* mutant mice. We also showed that *prx-1* and *prx-2* perform redundant functions in the mandibular process of the first branchial arch mesenchyme. These genes are required for
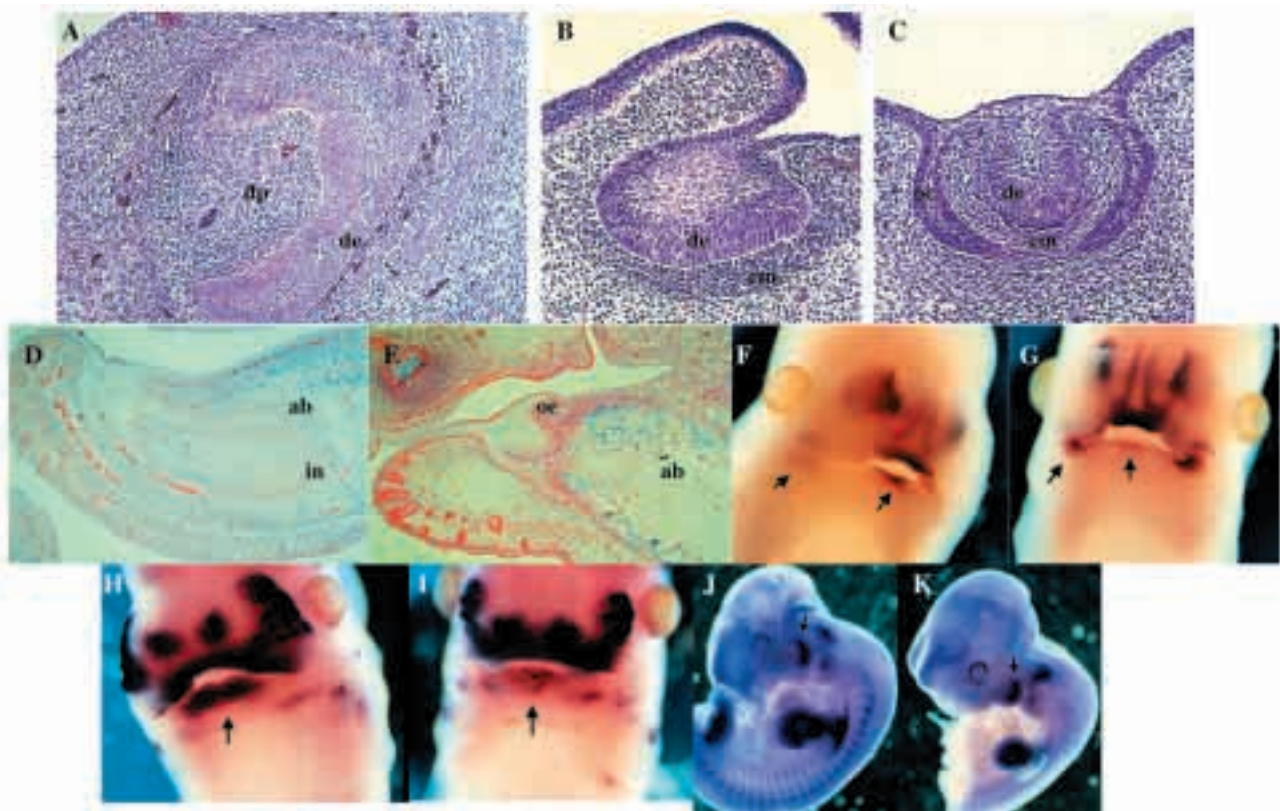

Fig. 6. Characterization of phenotypes within the mandibular process of *prx-1−/−; prx-2−/−* mutant mice. (A) Parasagittal section of 12.5 d.p.c. wild-type embryo through the bell-stage incisor tooth germ. At this point, a well-formed dental papilla (dp) has been surrounded by the dental epithelium (de). (B,C) In the double mutant, a parasagittal (B) and transverse (C) section at this time point demonstrates that the tooth germ has arrested at the bud stage. Although there is a condensed mesenchyme (cm) around the dental epithelium, the tooth germ has not progressed to the bell stage. (D,E) At 16.5 d.p.c., the incisor teeth (in) of the wild-type mouse (D) is a large structure that is embedded in alveolar bone (ab) while, in the double mutant (E), only a remnant of the normal incisor is evident and the position of this structure in relation to the alveolar bone is abnormal. Additionally, hypertrophy of the oral epithelium (oe) overlying the incisor tooth remnant is evident. (F,G) Whole-mount in situ at 12.5 d.p.c. using the *pax9* antisense probe demonstrates that *pax9* is expressed in the wild-type (F) dental mesenchyme of both the forming incisors and molars as denoted by the arrows. In the double mutant (G), expression of *pax9* was downregulated in the mandibular incisor while expression was maintained in the molars (arrows). (H,I) Whole-mount in situ at 12.5 d.p.c. using the *patched* probe demonstrated that *patched* was expressed at high levels in the developing wild-type incisors (H) but was downregulated in the double mutant mandibular incisors (I). (J,K) Whole-mount in situ at 11.5 d.p.c. using the *sox9* probe. Both the wild-type (J) and the double mutant (K) embryos demonstrate expression in the mandibular process at this stage (arrows). ab, alveolar bone; cm, condensing mesenchyme; de, dental epithelium; dp, dental papilla; in, incisor tooth; oe, oral epithelium.

Fig. 7. Cells which are fated to express *prx-1* are found in ectopic locations in *prx-1ⁿᵉᵒ–/–; prx-2–/–* embryos. (A,B) Expression of the *prx-1 2.7 lacZ* transgene that marks a subpopulation of *prx-1*-expressing cells in the craniofacial primordia. At 11.0 d.p.c., the wild-type embryo does not yet express this transgene in the branchial arches, although expression is detected in the limb buds. *lacZ* expression in the posterior regions of the head is ectopic staining associated with this transgene construct in all lines analyzed. (B) *lacZ*-expressing cells are detected in the maxillary (mx) and mandibular (md) processes as well as the hyoid arch at 11.0 d.p.c. in the double mutant embryos (arrows). (C) At 12.5 d.p.c., expression of the *prx-1 2.7 lacZ* transgene is detected in cells at the lateral aspect of the forming maxilla and in a group of cells at the distal aspect of the forming mandible which are obscured in this lateral view. (D) In the double mutant embryo at this stage, *lacZ* expression is detected in the maxilla and mandible as well as in two ectopic locations, caudally in the hyoid arch derived cells and in cells that will contribute to the external ear structures (arrows). e, eye; md, mandibular process; mx, maxillary process.
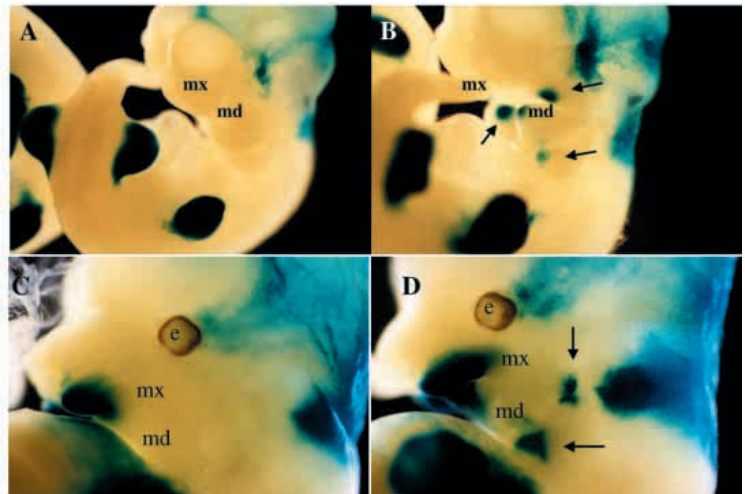
formation of the mandibular incisor and the rostral mandible, as well as the majority of Meckel's cartilage. Using a transgene that distinguishes between subpopulations of *prx-1*-expressing cells in the craniofacial primordia, we showed that *prx-1*-expressing cells are found at ectopic locations in the double mutant mice. Taken together, our data demonstrate that the *prx-1* and *prx-2* genes function to maintain and stabilize cell fates of craniofacial mesenchyme.

Cells fated to express *prx-1* are lost from the structures that are defective in the *prx-1* mutant mouse
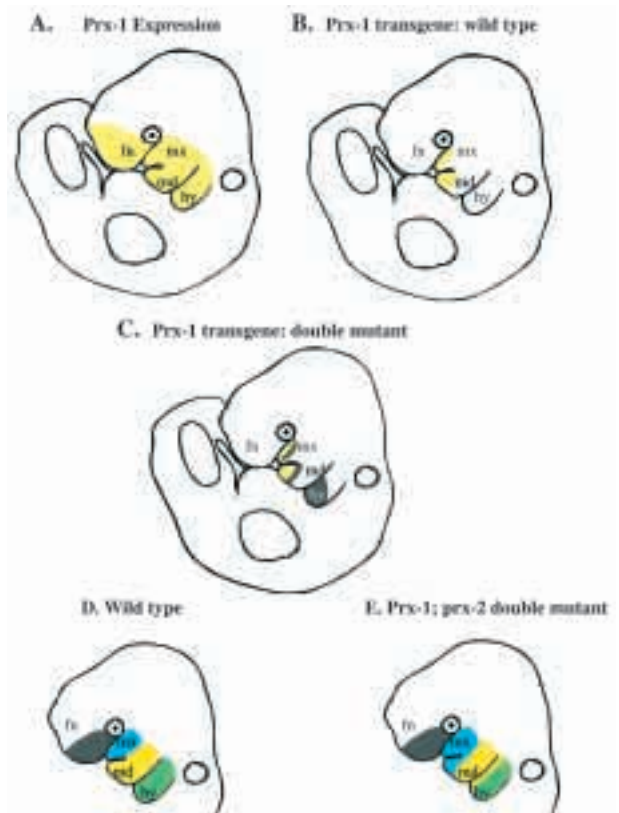
The *prx-1ⁿᵉᵒ* mutant mouse had craniofacial defects that were confined to cells within the proximal aspect of the first branchial arch (Martin et al., 1995). We now show that cells that are fated to express *prx-1* are allocated normally to the precursors of the defective structures. *lacZ*-positive cells were found at normal locations up until 11.5 d.p.c. However, at 12.5 d.p.c., we noted that *lacZ*-expressing cells were absent in structures derived from the maxillary process of the first branchial arch. From this, we conclude that *prx-1* is required for maintenance of cell fates within this region of the first branchial arch mesenchyme. In the absence of *prx-1* function, specific populations of cells are present but fail to express *lacZ*.

Fig. 8. Diagram of developmental fate of cells that normally express *prx-1* in wild-type and mutant backgrounds. (A-C) The entire *prx-1*-expressing field at 11.0 d.p.c. within the craniofacial region of a wild-type mouse (A) (shaded yellow). (B) The subpopulation of *prx-1*-expressing cells that normally express the *prx-1 2.7 lacZ* transgene in the wild-type mouse at 11.0 d.p.c. (shaded yellow). (C) The change in expression of the *prx-1 2.7 lacZ* transgene in the double mutant background. Note that aberrantly expressing cells (shaded gray) are found in the hyoid arch. The gray cells surrounding the yellow in the maxillary and mandibular processes signify cells that prematurely activated the transgene. (D,E) In the wild type (D), *prx-1*-expressing cells are found in all facial prominences however, these cells are developmentally distinct (as denoted by the different colors). In the double mutant background (E), cell fates are reprogrammed such that cells in the hyoid arch (shaded green) now take on the properties of cells within the mandibular processes (shaded yellow). Fn, frontonasal process; hy, hyoid arch; md, mandibular process; mx, maxillary process.

Alternatively, these same cells may be lost either by failing to proliferate or by activating apoptotic programs. Lineage-tracing experiments using chimeric analysis are now underway to distinguish between these two possibilities.

prx-1 and *prx-2* perform redundant functions in the mandibular process of the first branchial arch

The cranial abnormalities observed in the *prx-1ⁿᵉᵒ* mutant were confined to the proximal aspect of the first branchial arch (Martin et al., 1995). Thus, despite widespread expression in other regions of the forming craniofacial skeleton, no function for *prx-1* was observed. We have found that *prx-1ⁿᵉᵒ; prx-2*

double mutants had severe defects in structures derived from the mandibular process of the first branchial arch, demonstrating that these two genes perform redundant functions in the distal mandibular arch precursors. In double mutants, the rostral aspect of the mandible was fused and the mandibular incisor arrested as a bud-stage tooth germ. Additionally, Meckel's cartilage was severely deficient.

In order to gain insight into the molecular mechanisms underlying the incisor tooth defect, we studied the expression of two genes that are components of signaling pathways that have been implicated in tooth organogenesis. Expression of *Pax9,* an early marker for tooth development, was downregulated in the double mutant tooth germs. Function of *pax9* is required for progression of tooth development past the bud stage (Neubuser et al., 1997). In addition, *pax9* has been proposed to determine placement of tooth bud initiation by integrating *FGF* and *BMP* signaling pathways (Neubuser et al., 1997). *prx-1^{neo}; prx-2* double mutant incisors also arrested at the bud stage as a single incisor instead of the usual two. These data suggest that *prx-1* and *prx-2* function to maintain *pax9* expression in the forming mandibular incisor. Downregulated expression of *patched* in the double mutant incisors also supports the notion that *prx-1* and *prx-2* are required for the maintenance of normal signaling pathways required for mandibular incisor tooth formation.

Although formation of Meckel's cartilage in the double mutants was severely disrupted, we found that expression of *sox9* in the mandibular process of double mutant embryos was intact prior to chondrogenesis at 11.5 d.p.c. Therefore, although the chondrogenic mesenchyme was correctly specified, it failed to be maintained and complete its developmental program.

prx-1-expressing cells are found in ectopic locations in the *prx-1^{neo}; prx-2* double mutant mice

We have made use of the *prx-1 2.7 lacZ* transgene that distinguishes between subpopulations of *prx-1*-expressing cells in the craniofacial primordia. In the double mutant embryos, we found ectopic expression of this transgene. Cells that did not express the transgene in wild-type embryos were reprogrammed to express in the double mutant. Aberrant expression of this transgene in the double mutant included cells that did not normally express, as well as cells that prematurely expressed the transgene. These data suggest that *prx-1* and *prx-2* function to maintain or stabilize cell fates in the post migratory cranial mesenchyme.

We believe these data provide insight into the developmental basis for the craniofacial phenotypes observed in both the *prx-1* single mutant and the *prx-1; prx-2* double mutant mice. Although *prx-1*-expressing cells are found in all facial primordia, these cells are not developmentally equivalent (Fig. 8A,D). Cells within the maxillary prominence respond to different positional cues than cells within the mandibular process. The *prx-1 2.7 lacZ* transgene marking experiment demonstrated that in double mutants, cells within the *prx-1*-expressing field have been reprogrammed (Fig. 8A-C). Thus, in double mutant embryos, hyoid arch mesenchyme expresses a transgene that, in the wild-type embryo, would only be expressed in the maxillary and mandibular processes of the first branchial arch. We propose that this reprogramming of the craniofacial primordia in single *prx-1* mutant and *prx-1; prx-2*

double mutant embryos underlies the observed craniofacial phenotypes. The consequence of this change in cell fate is that subpopulations of cranial mesenchyme receive inappropriate positional information to which they cannot respond resulting in failure to maintain gene expression in forming craniofacial organs (Fig. 8E).

Our results have important implications for the developmental mechanisms underlying craniofacial development. Recent work has demonstrated that the CNC has some degree of intrinsic patterning capacity (Couly et al., 1998). Our data suggest that *prx-1* and *prx-2* are components of the genetic program that functions to maintain this patterning information during the postmigratory phases of craniofacial organogenesis

REFERENCES

Beddington, R. S., Morgernstern, J., Land, H. and Hogan, A. (1989). An in situ transgenic enzyme marker for the midgestation mouse embryo and the visualization of inner cell mass clones during early organogenesis. *Development* **106,** 37-46.

Cheng, T. C., Wallace, M. C., Merlie, J. P. and Olson, E. N. (1993). Separable regulatory elements governing myogenin transcription in mouse embryogenesis. *Science* **261,** 215-218.

Couly, G. F., Coltey, P. M. and Le Douarin, N. M. (1993). The triple origin of skull in higher vertebrates: a study in quail-chick chimeras. *Development* **117,** 409-429.

Couly, G., Grapin-Botton, A., Coltey, P. and Le Douarin, N. M. (1996). The regeneration of the cephalic neural crest, a problem revisited: the regenerating cells originate from the contralateral or from the anterior and posterior neural fold. *Development* **122,** 3393-407.

Couly, G., Grapin-Botton, A., Coltey, P., Ruhin, B. and Le Douarin, N. M. (1998). Determination of the identity of the derivatives of the cephalic neural crest: incompatibility between Hox gene expression and lower jaw development. *Development* **125,** 3445-59.

Cserjesi, P., Lilly, B., Bryson, L., Wang, Y., Sassoon, D. A. and Olson, E. N. (1992). MHox: a mesodermally restricted homeodomain protein that binds an essential site in the muscle creatine kinase enhancer. *Development* **115,** 1087-1101.

Edmondson, D. G., Lyons, G. E., Martin, J. F. and Olson, E. N. (1994). Mef2 gene expression marks the cardiac and skeletal muscle lineages during mouse embryogenesis. *Development* **120,** 1251-63.

Goodrich, L. V., Johnson, R. L., Milenkovic, L., McMahon, J. A. and Scott, M. P. (1996). Conservation of the hedgehog/patched signaling pathway from flies to mice: induction of a mouse patched gene by Hedgehog. *Genes Dev.* **10,** 301-312.

Helms, J. A., Kim, C. H., Hu, D., Minkoff, R., Thaller, C. and Eichele, G. (1997). Sonic hedgehog participates in craniofacial morphogenesis and is down-regulated by teratogenic doses of retinoic acid. *Dev. Biol.* **187,** 25-35.

Kern, M. J., Witte, D. P., Valerius, M. T., Aronow, B. J. and Potter, S. S. (1992). A novel murine homeobox gene isolated by a tissue specific PCR cloning strategy. *Nucleic Acids Res.* **20,** 5189-5195.

Kuratani, S., Martin, J. F., Wawersik, S., Lilly, B., Eichele, G. and Olson, E. N. (1994). The expression pattern of the chick homeobox gene gMHox suggests a role in patterning of the limbs and face and in compartmentalization of somites. *Dev. Biol.* **161,** 357-369.

Le Douarin, N. M., Ziller, C. and Couly, G. F. (1993). Patterning of neural crest derivatives in the avian embryo: in vivo and in vitro studies. *Dev. Biol.* **159,** 24-49.

Leussink, B., Brouwer, A., El Khattabi, M., Poelmann, R. E., Gittenberger-de Groot, A. C. and Meijlink, F. (1995). Expression patterns of the paired-related homeobox genes *MHox/Prx1* and *S8/Prx2* suggest roles in development of the heart and the forebrain. *Mech. Dev.* **52,** 51-64.

Lu, M., Cheng, H. T., Lacy, A., Kern, M. J., Argao, E. A., Potter, S. S., Olson, E. N. and Martin, J. F. (1998). *Paired*-related homeobox genes cooperate in handplate and hindlimb zeugopod morphogenesis. *Dev. Biol.*, in press.

Mansour, S. L., Thomas, K. R. and Capecchi, M. R. (1988). Disruption of the proto-oncogene int-2 in mouse embryo-derived stem cells: a general strategy for targeting mutations to non-selectable genes. *Nature* **336,** 348-352.

Marigo, V., Scott, M. P., Johnson, R. L., Goodrich, L. V. and Tabin, C. J. (1996). Conservation in hedgehog signaling: induction of a chicken patched homolog by Sonic hedgehog in the developing limb. *Development* **122,** 1225-1233.

Martin, J. F., Bradley, A. and Olson, E. N. (1995). The *paired*-like homeobox gene *MHox* is required for early events of skeletogenesis in multiple lineages. *Genes Dev.* **9,** 1237-1249.

McMahon, A. P. and Bradley, A. (1990). The Wnt-1 (int-1) proto-oncogene is required for development of a large region of the mouse brain. *Cell* **62,** 1073-1085.

Neubuser, A., Peters, H., Balling, R. and Martin, G. R. (1997). Antagonistic interactions between FGF and BMP signaling pathways: a mechanism for positioning the sites of tooth formation. *Cell* **90,** 247-255.

Noden, D. M. (1988). Interactions and fates of avian craniofacial mesenchyme. *Development* **103,** 121-140.

Opstelten, D. J., Vogels, R., Robert, B., Kalkhoven, E., Zwartkruis, F., de Laaf, L., Destree, O. H., Deschamps, J., Lawson, K. A. and Meijlink, F. (1991). The mouse homeobox gene, S8, is expressed during embryogenesis predominantly in mesenchyme. *Mech. Dev.* **34,** 29-41.

Ramirez-Solis, R., Rivera-Perez, J., Wallace, J. D., Wims, M., Zheng, H. and Bradley, A. (1992). Genomic DNA microextraction: a method to screen numerous samples. *Anal. Biochem.* **201,** 331-335.

Scott, M. P. (1992). Vertebrate homeobox gene nomenclature [letter]. *Cell* **71,** 551-3.

Thomas, B. L., Tucker, A. S., Qui, M., Ferguson, C. A., Hardcastle, Z., Rubenstein, J. L. and Sharpe, P. T. (1997). Role of Dlx-1 and Dlx-2 genes in patterning of the murine dentition. *Development* **124,** 4811-4818.

Zhao, Q., Eberspaecher, H., Lefebvre, V. and De Crombrugghe, B. (1997). Parallel expression of Sox9 and Col2a1 in cells undergoing chondrogenesis. *Dev. Dyn.* **209,** 377-386.